Anisotropic collective charge excitations in quasi-metallic two-dimensional transition-metal dichalcogenides

Chi Sin Tang†, Xinmao Yin†,, Ming Yang†, Di Wu, Jing Wu, Lai Mun Wong, Changjian Li, Shi Wun Tong, Yung-Huang Chang, Fangping Ouyang, Yuan Ping Feng, Shi Jie Wang, Dongzhi Chi, Mark B. H. Breese, Wenjing Zhang, Andrivo Rusydi, Andrew T. S. Wee**

C. S. Tang, Dr. X. Yin, Prof. Y. P. Feng, Prof. M. B. H. Breese, Prof. A. Rusydi, Prof. A. T. S. Wee
Department of Physics, Faculty of Science, National University of Singapore, S12 Science Drive 3, 117551, Singapore
Email: phyyxm@nus.edu.sg, phyweets@nus.edu.sg

D. Wu, Prof. W. Zhang
International Collaborative Laboratory of 2D Materials for Optoelectronics Science and Technology, Shenzhen University, Shenzhen 518060, China

Dr. M. Yang, Dr. J. Wu, Dr. L. M. Wong, Dr. S. W. Tong, Prof. S. J. Wang, Dr. D. Chi
Institute of Materials Research and Engineering (IMRE), A*STAR (Agency for Science, Technology and Research), 2 Fusionopolis Way, Innovis, 138634, Singapore

Dr. C. Li
Department of Materials Science & Engineering, National University of Singapore, 9 Engineering Drive 1, Singapore 117575, Singapore

Dr. X. Yin, Prof. M. B. H. Breese, Prof. A. Rusydi
Singapore Synchrotron Light Source (SSLS), National University of Singapore, 5 Research Link, 117603, Singapore

C. S. Tang, Prof. A. T. S. Wee
NUS Graduate School for Integrative Sciences and Engineering, National University of Singapore, 21 Lower Kent Ridge, 119077, Singapore

D. Wu, Prof. F. Ouyang
School of Physics and Electronics, Central South University, No. 932, South Lushan Road, Changsha, Hunan Province 410083, China

Prof. Y. Chang
Bachelor Program in Interdisciplinary Studies, National Yunlin University of Science and Technology, 123 University Road, Section 3, Douliou, Yunlin 64002, Taiwan

Keywords: Plasmon, Phase transition, Transition-metal dichalcogenide, Spectroscopic ellipsometry, Anisotropic charge dynamics

*Correspondence to phyyxm@nus.edu.sg (X.Y.), phyweets@nus.edu.sg (A.T.S.W.).

†These authors contributed equally to this work.

The quasi-metallic 1T'-phase two-dimensional transition-metal dichalcogenides (2D-TMDs) consist of one-dimensional zigzag metal chains stacked periodically along a single axis. This gives rise to its prominent physical properties which promises the onset of novel physical phenomena and applications. Here, we explore the in-plane electronic correlations and observe new mid-infrared plasmon excitations in 1T'-phase monolayer-WSe_2 and MoS_2 using optical spectroscopies. Based on an extensive first-principles study which analyzes the charge dynamics across multiple axes of the atomic-layered systems, the collective charge excitations is found to disperse only along the direction perpendicular to the chains. Further analysis reveals that the inter-chain long-range coupling is responsible for the coherent one-dimensional charge dynamics and the spin-orbit coupling affects the plasmon frequency. Detailed investigation to these charge collective modes in 2D-chained systems offers opportunities for novel device applications and has implications for the underlying mechanism that governs superconductivity in 2D-TMD systems.

Low-dimensional periodical patterned structures, such as two-dimensional layered systems or one-dimensional chain structures in higher dimensional materials, exhibit immensely intriguing wave phenomena due to the heavy influence by many-body interactions[1]. The highly-correlated collective modes take the place of single-particle excitations and detailed study of periodic materials kindles it as a burgeoning field of research spanning broad areas ranging from phononics, to photonics, plasmonics and magnonics[2-4]. A definitive example is the periodic CuO_2-planes in copper oxide-based (cuprate) systems where report is made that plasmon is induced via periodic inter-planar interactions and this distinct collective mode is argued to play a pivotal role in mediating high-temperature superconductivity[5]. Another notable example is the report of the periodic infinite-layer system $Nd_{0.8}Sr_{0.2}NiO_2$, of which, by

transforming the system from a pervoskite structure to a 2D periodic layered structure, a new superconductivity state is resulted in this nickelate system[6].

With the continuous exploration of two-dimensional transition-metal dichalcogenides (2D-TMDs), there arises novel high-performance devices based on their remarkable electronic and optoelectronic properties[7-9]. Beside the semiconducting 1H-phase 2D-TMDs, quasi-metallic 1T'-phase 2D-TMDs have particularly promised a range of new applications from supercapacitor electrodes[9] to hydrogen-based evolution reaction catalysts[7]. The in-plane atomic arrangement of 1T'-phase 2D-TMDs comprises a distorted sandwich structure, where the transition-metal atoms form a period-doubling 2×1 structure comprising 1D-zigzag chains[8]. This novel 1D-periodical structure gives rise to strong anisotropic properties that significantly influence the electronic properties of 2D-TMDs. For instance, alongside the influences of spin-orbit coupling and electronic correlations, the anisotropic structure results in a band inversion around the Γ-point near the Fermi level which leads to the fundamental and inverted gap opening[8]. Distinct possibilities emerge in uncovering new physical phenomena in this unique structural phase. Specifically, unanswered questions remain on how 1D-chain structures affect the charge dynamics of 1T'-phase 2D-TMDs. With reports suggesting additional quasiparticle interactions can create strong-correlate-configurations yielding new phenomena such as Mott insulating system[10], superconductivity and pseudogap phases in high-temperature superconductors[11]. Hence, it is vital to probe the quasiparticle dynamics in 1T'-phase 2D-TMDs and unravel their correlated electronic properties.

Here, we report the direct observation of new mid-infrared plasmons in 1T'-phase monolayer-WSe_2 and MoS_2 which are absent from their semiconducting 1H-phase counterparts. First-principles investigation demonstrates that these plasmons are anisotropic–while they are present in the direction perpendicular to the zigzag transition-metal chain (*y*-direction, **Figure** 1a and 1b), they are absent along the zigzag chain. With the photon-in-photon-out and photon

energy specific methodology of high-resolution spectroscopic ellipsometry, it is a premier technique to directly probe the plasmon modes (Figure 1c) where sample charging and higher harmonic processes can be ruled out. We deduce that coupling between the zigzag transition-metal chains is the key mechanism driving the collective charge dynamics along the *y*-direction (Figure 1b). Analysis indicates the significant role of the plasmons in the charge dynamics of 2D-TMD quantum structures and mediating the onset of superconductivity reported in 1T'-phase 2D-TMDs[12]. This work also unveils the influence of spin-orbit coupling (SOC) in regulating the plasmon energy and establishes an link between the chain structure and 1D-charge dynamics in 1T'-phase 2D-TMDs.

Phase engineering techniques have made 1T'-phase 2D-TMDs greatly accessible via various processes such as the *n*-butyl lithium (*n*-BuLi) treatment[13]. However, large-area full-covered 1T'-phase 2D-TMDs are more favourable for the effective characterization of its ordered 1D-chain structure via spectroscopic techniques. An annealing-based technique for a high-yield 1H-1T' phase transition of large-area CVD-grown 2D-TMDs has recently been reported, where spectroscopic ellipsometry, Raman and photoluminescence spectroscopy are employed to confirm the different structural phases[13]. Besides, this study has further indicated that that electron-doping from the metallic substrate, facilitated by interfacial tensile strain, plays a very significant role in the induction of the 1H-to-1T' phase-transition of 2D-TMDs[14]. Prior study has reported that monolayer-WSe_2/Au annealed at the temperature region of ~500-550K enables a ~59% yield of 1T'-phase monolayer-WSe_2[15].

High-quality large-area monolayer-WSe_2 samples are synthesized on sapphire substrate (detail in Supllementary). Each sample is annealed at the respective temperature in a high-vacuum chamber with a base pressure of 1×10^{-9} mbar for ~15mins. Thereafter, the sample is naturally cooled to room temperature before the measurement. Similar to previous reports[15],

confirmation of the 1H-1T' phase transition of monolayer-WSe_2 on gold substrate is provided via a systematic annealing temperature-dependent photoluminescence (PL), Raman, high-resolution transmission electron microscopy (HRTEM) and UV-Vis spectroscopic ellipsometry study. The characterization data of monolayer-WSe_2/Au using these three techniques are displayed in **Figure** 2a,b,c (details in Supporting Information). The inverted and fundamental gaps are important features for 1T'-phase 2D-TMDs[8]. PL data shows the weakening exciton peaks (Figure 2a), the corresponding appearance of the characteristic 1T'-phase Raman modes (Figure 2b) and the 1T'-phase inverted gap feature (Figure 2c) take place mainly after annealing at 500K (details in Supporting Information). It is important to highlight that the broad mid-gap feature at ~1600nm from the UV-Vis spectroscopic ellipsometry data (Figure 2c) has contributions from both the 1T'-phase inverted gap and the presence of charge-lattice interaction at the interface[14]. While thermal decomposition begins after sample annealing at 550K (Figure 2d), interfacial strain and electron doping by the Au substrate on the monolayer are still present. Therefore, there is still a small broad mid-gap feature at ~1600nm after annealing at 550K.

Further confirmation of the 1H-1T' transition is made via HRTEM characterization that compares molecular configuration before and after the annealing process at 500K (details in Supporting Information). Apart from confirming the 1H-1T' structural phase transition of the monolayer sample, these experiments further affirms the good monolayer crystalline property in its pristine state and after the annealing process. Figure 2d displays the optical conductivity, σ_1, of monolayer-WSe_2/Au in its as-prepared state and after annealing at 500 and 550K, respectively. A strong peak feature with maximum intensity at ~14.4μm (~0.09eV) appears after annealing at 500K but disappears after annealing at 550K. This peak position is in agreement with the calculated fundamental gap size of ~0.08eV (~15μm) for 1T'-phase WSe_2 [8]. While 1T'-phase monolayer-WSe_2 is present after annealing at 500K, the start of thermal

decomposition brought about by high heat leads to the disappearance of the fundamental gap after annealing at 550K. This is an indication that the fundamental gap feature is easily affected by decomposition and defects due to its proximity to the Fermi Level. The 1H-1T' phase transition is confirmed via the direct observation of the inverted and fundamental gaps. Furthermore, this annealing temperature is consistent with previous studies where ~500K is near the optimum temperature for the 1H-1T' phase transition of WSe_2/Au[14, 15].

Having confirmed the 1T'-phase monolayer-WSe_2 after sample annealing at 500K, we analyse the ε_1 spectra (Figure 2e) simultaneously with its loss function (LF) spectra (Figure 2f). Unlike the as-prepared state, the LF spectrum registers a distinct main peak at ~12.7μm that is absent from the σ_1 and ε_1 spectra (Figure 2d and 2e), which also coincides with the zero-crossing of the corresponding ε_1 spectrum at ~12.8μm (Figure 2f). To understand these optical features in the LF spectra, we consider the phenomenon of plasmon excitation– quantum of collective charge excitation arising from interactions between electromagnetic fields and charges[16]. Such intense collective charge excitation manifests itself as a prominent peak in the LF spectrum at a characteristic plasma frequency, ω_P, which depends on the carrier density and the media's complex dielectric response. The presence of a zero-crossing in the real dielectric function component, $\varepsilon_1(\omega_p)=0$, confirms the presence of the intense plasmon mode[16]. The collective optical features in both LF and ε_1 spectra of 1T'-phase WSe_2/Au strongly suggest the appearance of a plasmon mode in the mid-infrared regime at ~12.7μm. Note that the slight disparity between the significant LF peak and the ε_1 zero-crossing positions is attributed to charge scattering present with the two-dimensional lattice.

Plasmon excitations are generally reported in metals[17], including graphene[18] where Drude responses are observed. For metals, the plasma frequency is usually located in the ultraviolet regime[17], while electromagnetic waves with frequency above the plasma frequency is

transmitted because the electrons in the material are unable to respond swiftly enough to screen, light frequencies below the plasma frequency are reflected due to the electrodynamical interaction with the material where the electric field is screened by the electrons. Interestingly, this monolayer-WSe_2 system comprises both 1H-phase (with bandgap of ~1.6eV) and 1T'-phase structure (with fundamental gap of ~0.09eV), does not have a Drude response (Figure 2d), indicating that our sample is not truly metallic but possesses a mid-infrared plasmon. Hence, the experimentally observed plasmon excitation at ~12.7μm may be associated with the 1T'-phase anisotropic structure. A comprehensive first-principles study is conducted to substantiate the connection between the anisotropic 1T'-phase WSe_2 structure and the new mid-infrared plasmon.

Fitting analyses show that the plasmon peak widths (detail in Supporting Information and Table S1) are similar to those reported in noble metals[17] and graphene nanostructures[19]. Interestingly, the dephasing time, *T*, of these plasmons are significantly higher than those of other systems (detail in Supporting Information)[19, 20]. This suggests the 1T'-phase 2D-TMD system is less prone to plasmonic dissipation and other charge scattering processes due to interactions with lattice and site defects. Hence, such monolayer systems hold potential for low-loss novel device applications. Besides, such analyses to charge scattering in 2D-TMDs are pivotal to the understanding of possible mitigating factors to reduce plasmonic dissipation and losses.

To further confirm this observation, first-principles calculations are performed. **Figure** 3a and 3b display the calculated ε_1 and LF spectra of 1T'-phase monolayer-WSe_2 with SOC effects accounted for (details in Supplmentary). While Figure 3a displays a zero-crossing at ~4.13μm, importantly, a prominent peak is noticeable in the calculated LF spectrum (Figure 3b) which resolves the 1T'-phase monolayer-WSe_2 plasmon along the zigzag transition-metal chain

direction (*x*-direction) and the direction perpendicular to it (*y*-direction) depicted in Figure 1b. Interestingly, while no feature is observed along the *x*-direction, this prominent peak is present along the *y*-axis at ~4.6μm. This is a substantial theoretical proof of the new mid-infrared plasmon in 1T'-phase monolayer-WSe_2. With no other peaks present at longer wavelength (lower energy close to Fermi level, Figure 3b inset), it suggests further agreement with the experimentally observed mid-infrared plasmon in 1T'-phase monolayer-WSe_2. Besides, the result provides strong evidence that this plasmon possesses anisotropic features– it only occurs in the direction perpendicular to the zigzag transition-metal chain.

Discrepancy of the plasmon position between the experimental and first-principles study is attributed to the sample's intrinsic defects and interfacial localized strain which distorts the regular zigzag 1T' chains due to the non-uniform interactions with the metallic substrate and SOC effects[14, 21]. The blue-shift in the plasmon peak position of monolayer-WSe_2 without SOC effects (Figure S3) shows that the disparity in plasmon position with experimental result further increases by blue-shifting to ~3.6μm. This demonstrates how SOC affects the plasmon energy of 2D-TMDs. Besides, the optoelectronic features of the monolayer-WSe_2 are tunable by intrinsic film defects and effects of localized interfacial lattice strain while the first-principles study models a perfect 2D-lattice.

Recently, the inter-planar Coulomb interaction and 2D-charge dynamics are identified as causes for the coherent acoustic plasmon in cuprate superconductors[5]. This long-range coupling between the CuO_2-planes and the propagation of the plasmons is suggested to play a crucial role in mediating superconductivity. With the interlayer coupling between 2D-CuO_2-planes in 3D-cuprate lattices, such analogous phenomenon involving reduced dimensionality is also noticeable here where coupling between 1D-zigzag chains in 2D-TMDs occurs. Hence, the coupling between zigzag transition-metal chains in 1T'-phase monolayer-WSe_2 drives the

collective 1D-charge dynamics (Figure 1a) which eventually results in the plasmon. The notion that long-range inter-chain coupling leads to plasmon formation is further substantiated by reports that long-range electronic correlations leads to the appearance of plasmons in other strongly-correlated systems[22].

Having confirmed the mid-infrared plasmon in 1T'-phase monolayer-WSe_2, we further demonstrate that it also appears in other 1T'-phase 2D-TMDs where similar experimental process is conducted on 1T'-phase monolayer-MoS_2. 1H-1T' phase transition for monolayer-MoS_2/Au is confirmed via PL, Raman spectroscopy and spectroscopic ellipsometry displayed in **Figure** 4a,b,c (detail in Supporting Information). Spectroscopic ellipsometry results show the appearance of the inverted gap (1T'-phase) as a mid-gap peak (Figure 4c). Figure 4d,e,f display the optical conductivity, dielectric function, and LF, of monolayer-MoS_2/Au in its as-prepared state and after annealing at 500 and 550K characterized using infrared-range Spectroscopic ellipsometry.

In its as-prepared state, the σ_1 spectrum of monolayer-MoS_2/Au is consistent with a previous study [14]. By annealing the sample at 500K, a peak appears at ~11.5μm (colour-coded arrows in Figure 4d). While the peak intensity reduces after annealing at 550K, it persists at the same wavelength. Similar to previous annealing-based study, this peak is attributed to the fundamental gap that is formed due to the phase transition[14]. The fundamental gap position at ~11.5μm (~0.1eV) is consistent with the previous theoretical study of monolayer-MoS_2[8]. Observations of both the inverted and fundamental gaps confirmed the phase transition.

Having ascertained the presence of the 1T'-phase monolayer-MoS_2 after annealing, analysis of the ε_1 and LF spectra (Figure 4e and 4f, respectively) was performed to demonstrate the presence of the plasmon mode. After annealing at 500K, the ε_1 spectrum zero-crossing is

observed at ~16.3μm (Figure 4e) alongside the appearance of a main broad LF peak at ~16.2μm which is absent from both the ε_1 and σ_1 spectra. After annealing at 550K, the main LF peak is red-shifted to ~17.7μm while the ε_1 zero-crossing at ~18.1μm. Hence, the mid-infrared plasmon is also present in 1T'-phase monolayer-MoS_2. Table S1 summarizes the plasmon fitting properties for both 1T'-phase monolayer-WSe_2 and MoS_2. Note the plasmon energy of WSe_2 (~12-13μm) is higher than that of MoS_2 (~16-18μm), with the SOC strength directly related to the atomic mass of the constituent atoms[23], SOC effects is stronger in monolayer-WSe_2 than monolayer-MoS_2. Hence, SOC effects may play a crucial role in plasmon formation and in determining its position.

This study holds important implications in unravelling the mechanism governing superconductivity in 1T'-phase 2D-TMDs[12, 24]. Multiple models are proposed to identify the mechanism providing the 'pairing glue' for the formation of electron pairs that mediates superconductivity. For instance, the role of phonons in charge-lattice interactions[25] or magnons in spin fluctuations[11] have been considered as the 'pairing glue'. With suggestions of inter-planar plasmons in multilayer cuprates mediating high-temperature superconductivity[26], we postulate that plasmons in 1T'-phase 2D-TMDs could facilitate the electron-plasmon interaction mechanism to form electron pairs that possibly underlies their superconductive properties[12, 24] (details in Supporting Information). This is further substantiated by reports made that 1D-chains have been associated with superconductivity[27, 28].

Overall, we provide an exceptional opportunity to study the 1D-behavior of mid-infrared plasmons in monolayer-WSe_2 and MoS_2 unique to their 1T'-phase. While 1H-1T' phase transition is achieved via our annealing technique, the reverse process is also readily

accessible[13, 29]. Therefore, the ease of regulating the 1H-1T'-phases in 2D-TMDs allows one to tune this system as a mid-infrared plasmon on/off-switch detector. Thus, it serves as an effective plasmonic photodetector which promises novel nano-plasmonic applications and other heterostructure engineering devices in the optical and near-infrared regime. This new mid-infrared plasmon open a new way in the fabrication of optoelectronic devices where plasmons can be exploited in multiple scientific and engineering applications, as compared to the plasmons in normal metals which are usually found in the ultraviolet range. Further analysis suggests that collective charge dynamics is induced by the long-range coupling between the zigzag transition-metal chains in 1T'-phase 2D-TMDs. This unravels the role of long-range electronic correlations in 2D-TMD systems. In-depth study of the significantly higher plasmon dephasing times also provide clues to possible mitigating factors for reducing plasmonic dissipation and losses in 2D-TMD systems.

Supporting Information
Supporting Information is available from the Wiley Online Library or from the author.

Acknowledgements
Chi Sin Tang, Xinmao Yin and Ming Yang contributed equally to this work. We thank the Centre for Advanced 2D Materials (CA2DM) at the National University of Singapore in providing the necessary computing resources. We acknowledge the Singapore Synchrotron Light Source (SSLS) for providing the facilities necessary for conducting the experimental studies. The SSLS is a National Research Infrastructure under the National Research Foundation, Singapore. This work is financially supported by the National Natural Science Foundation of China (51472164), the Natural Science Foundation of SZU (000050), the 1000 Talents Program for Young Scientists of China, the Shenzhen Peacock Plan (KQTD2016053112042971), the Educational Commission of Guangdong Province (2015KGJHZ006), the Science and Technology Planning Project of Guangdong Province (2016B050501005), the China Postdoctoral Science Foundation funded project (2016M600664), the Singapore National Research Foundation under its Competitive Research Funding (NRF-CRP 8-2011-06 and NRF-CRP15-2015-01), MOE-AcRF Tier-2 (MOE2016-T2-2-110) and Singapore A*STAR 2D PHAROS project: 2D devices & materials for ubiquitous electronic, sensor and optoelectronic applications (SERC 1527000012).

Author contributions: C.S.T., X.Y., L.M.W. and S.J.W. performed spectroscopic ellipsometry measurements; D.W. F.O. and W.Z. prepared high-quality monolayer-films and performed Raman and Photoluminescence spectroscopic measurements; M.Y. and Y.P.F. carried out the first principles calculation; C.S.T., X.Y., and M.Y. analyzed the data and wrote the manuscript with assistance from all authors. X.Y. and A.T.S.W. conceived and supervised the project.

Received: ((will be filled in by the editorial staff))
Revised: ((will be filled in by the editorial staff))
Published online: ((will be filled in by the editorial staff))

References

[1] D. Boies, C. Bourbonnais, A. M. S. Tremblay, *Physical Review Letters* **1995**, *74*, 968.
[2] M. Maldovan, *Nature* **2013**, *503*, 209.
[3] A. V. Chumak, V. I. Vasyuchka, A. A. Serga, B. Hillebrands, *Nature Physics* **2015**, *11*, 453.
[4] P. Lodahl, S. Mahmoodian, S. Stobbe, A. Rauschenbeutel, P. Schneeweiss, J. Volz, H. Pichler, P. Zoller, *Nature* **2017**, *541*, 473.
[5] M. Hepting, L. Chaix, E. W. Huang, R. Fumagalli, Y. Y. Peng, B. Moritz, K. Kummer, N. B. Brookes, W. C. Lee, M. Hashimoto, T. Sarkar, J. F. He, C. R. Rotundu, Y. S. Lee, R. L. Greene, L. Braicovich, G. Ghiringhelli, Z. X. Shen, T. P. Devereaux, W. S. Lee, *Nature* **2018**, *563*, 374.
[6] D. Li, K. Lee, B. Y. Wang, M. Osada, S. Crossley, H. R. Lee, Y. Cui, Y. Hikita, H. Y. Hwang, *Nature* **2019**, *572*, 624.
[7] T. F. Jaramillo, K. P. Jørgensen, J. Bonde, J. H. Nielsen, S. Horch, I. Chorkendorff, *Science* **2007**, *317*, 100.
[8] X. Qian, J. Liu, L. Fu, J. Li, *Science* **2014**, *346*, 1344.
[9] M. Acerce, D. Voiry, M. Chhowalla, *Nature Nanotechnology* **2015**, *10*, 313.
[10] M. Endres, M. Cheneau, T. Fukuhara, C. Weitenberg, P. Schauß, C. Gross, L. Mazza, M. C. Bañuls, L. Pollet, I. Bloch, S. Kuhr, *Science* **2011**, *334*, 200.
[11] D. J. Scalapino, *Reviews of Modern Physics* **2012**, *84*, 1383.
[12] Y. Qi, P. G. Naumov, M. N. Ali, C. R. Rajamathi, W. Schnelle, O. Barkalov, M. Hanfland, S.-C. Wu, C. Shekhar, Y. Sun, V. Süß, M. Schmidt, U. Schwarz, E. Pippel, P. Werner, R. Hillebrand, T. Förster, E. Kampert, S. Parkin, R. J. Cava, C. Felser, B. Yan, S. A. Medvedev, *Nature Communications* **2016**, *7*, 11038.
[13] G. Eda, H. Yamaguchi, D. Voiry, T. Fujita, M. Chen, M. Chhowalla, *Nano Letters* **2011**, *11*, 5111.
[14] X. Yin, Q. Wang, L. Cao, C. S. Tang, X. Luo, Y. Zheng, L. M. Wong, S. J. Wang, S. Y. Quek, W. Zhang, A. Rusydi, A. T. S. Wee, *Nature Communications* **2017**, *8*, 486.
[15] X. Yin, C. S. Tang, D. Wu, W. Kong, C. Li, Q. Wang, L. Cao, M. Yang, Y.-H. Chang, D. Qi, F. Ouyang, S. J. Pennycook, Y. P. Feng, M. B. H. Breese, S. J. Wang, W. Zhang, A. Rusydi, A. T. S. Wee, *Advanced Science* **2019**, *6*, 1802093.
[16] D. Pines, *Reviews of Modern Physics* **1956**, *28*, 184.
[17] M. Rocca, F. Moresco, U. Valbusa, *Physical Review B* **1992**, *45*, 1399.
[18] A. N. Grigorenko, M. Polini, K. S. Novoselov, *Nature Photonics* **2012**, *6*, 749.
[19] H. Yan, T. Low, W. Zhu, Y. Wu, M. Freitag, X. Li, F. Guinea, P. Avouris, F. Xia, *Nature Photonics* **2013**, *7*, 394.

[20] J. van Wezel, R. Schuster, A. König, M. Knupfer, J. van den Brink, H. Berger, B. Büchner, *Physical Review Letters* **2011**, *107*, 176404.
[21] A. Allain, A. Kis, *ACS Nano* **2014**, *8*, 7180.
[22] E. G. C. P. van Loon, H. Hafermann, A. I. Lichtenstein, A. N. Rubtsov, M. I. Katsnelson, *Phys. Rev. Lett.* **2014**, *113*, 246407.
[23] F. Herman, C. D. Kuglin, K. F. Cuff, R. L. Kortum, *Physical Review Letters* **1963**, *11*, 541.
[24] C. Guo, J. Pan, H. Li, T. Lin, P. Liu, C. Song, D. Wang, G. Mu, X. Lai, H. Zhang, W. Zhou, M. Chen, F. Huang, *Journal of Materials Chemistry C* **2017**, *5*, 10855.
[25] J. Bardeen, L. N. Cooper, J. R. Schrieffer, *Physical Review* **1957**, *108*, 1175.
[26] V. Z. Kresin, H. Morawitz, *Physical Review B* **1988**, *37*, 7854.
[27] E. Berg, T. H. Geballe, S. A. Kivelson, *Physical Review B* **2007**, *76*, 214505.
[28] A. P. Petrović, D. Ansermet, D. Chernyshov, M. Hoesch, D. Salloum, P. Gougeon, M. Potel, L. Boeri, C. Panagopoulos, *Nature Communications* **2016**, *7*, 12262.
[29] S. S. Chou, Y.-K. Huang, J. Kim, B. Kaehr, B. M. Foley, P. Lu, C. Dykstra, P. E. Hopkins, C. J. Brinker, J. Huang, V. P. Dravid, *Journal of the American Chemical Society* **2015**, *137*, 1742.

Figures

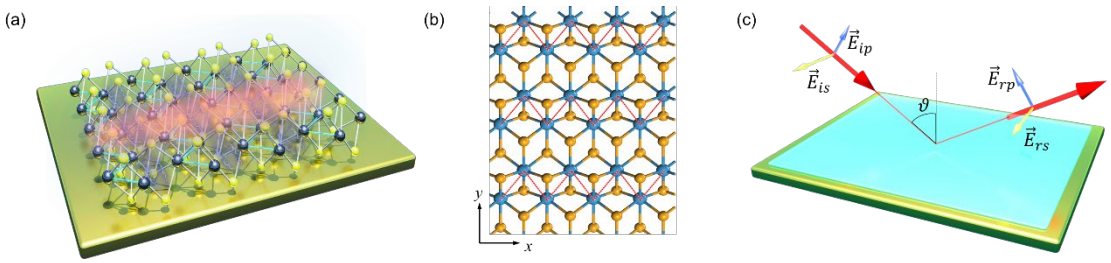

Figure 1. (a) Mid-infrared anisotropic plasmon in 1T'-phase WSe_2. (b) 1T'-phase monolayer-WSe_2 with its directional zigzag W structure traced by red dashed-lines. (c) Schematic of high-resolution spectroscopic ellipsometry to probe the mid-infrared optical properties of thin-film systems.

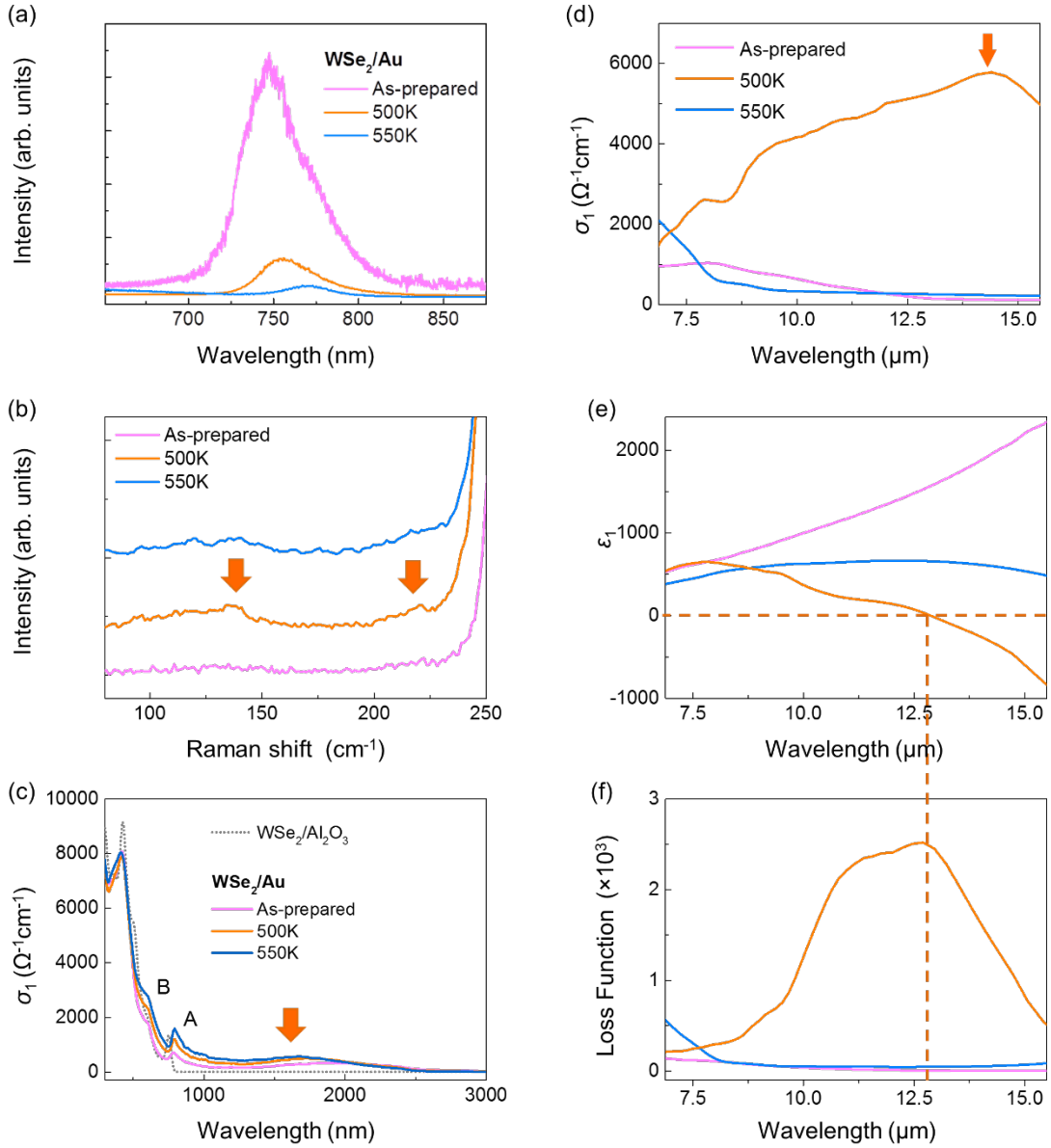

Figure 2. (a) PL data of the monolayer-WSe_2/Au sample. (b) Raman spectra where the orange arrows indicate the Raman features of 1T'-phase WSe_2 after annealing at 500K. (c) IR-to-visible range spectroscopic ellipsometry data where the orange arrow indicates the position of the inverted gap feature of 1T'-phase monolayer-WSe_2 after annealing at 500K. (d) Optical conductivity, σ_1, spectra of monolayer-WSe_2/Au sample with the orange arrow indicating the position of the fundamental gap of 1T'-phase monolayer-WSe_2 after annealing at 500K. (e) Dielectric function, ε_1, and (f) LF spectra of as-prepared monolayer-WSe_2/Au and after annealing at respective temperatures. Intersection of the orange dashed lines matches the zero-crossing position in the ε_1-spectrum (e) and the LF peak position (f).

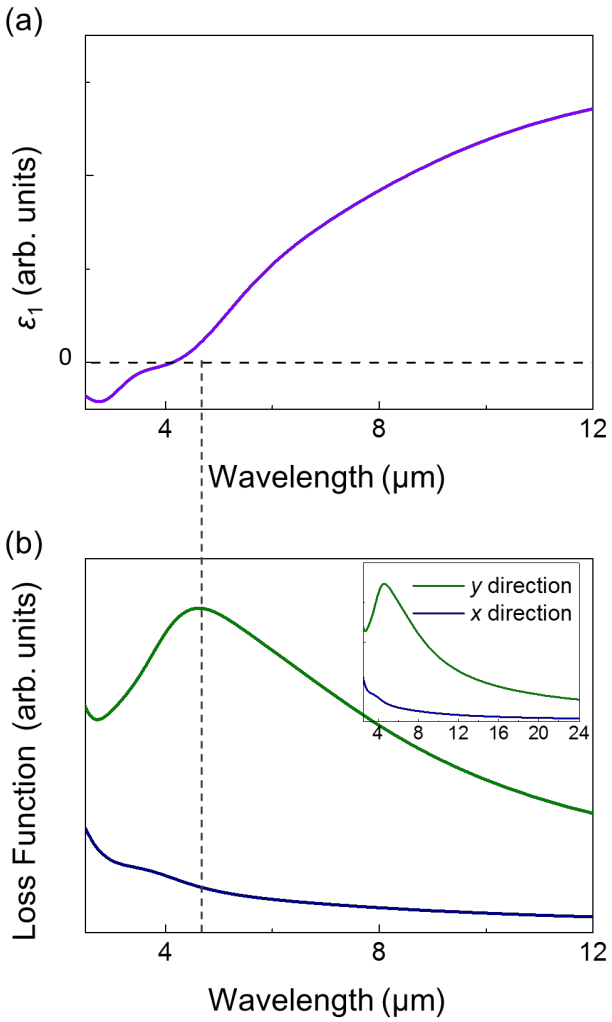

Figure 3. (a) ε_1, and (b) axis-dependent LF spectra derived via first-principles calculations (Inset: Calculated LF spectra extended to 18μm). Dashed-lines are visual guides to locate plasmon peak position with respect to the ε_1 spectrum zero-crossing.

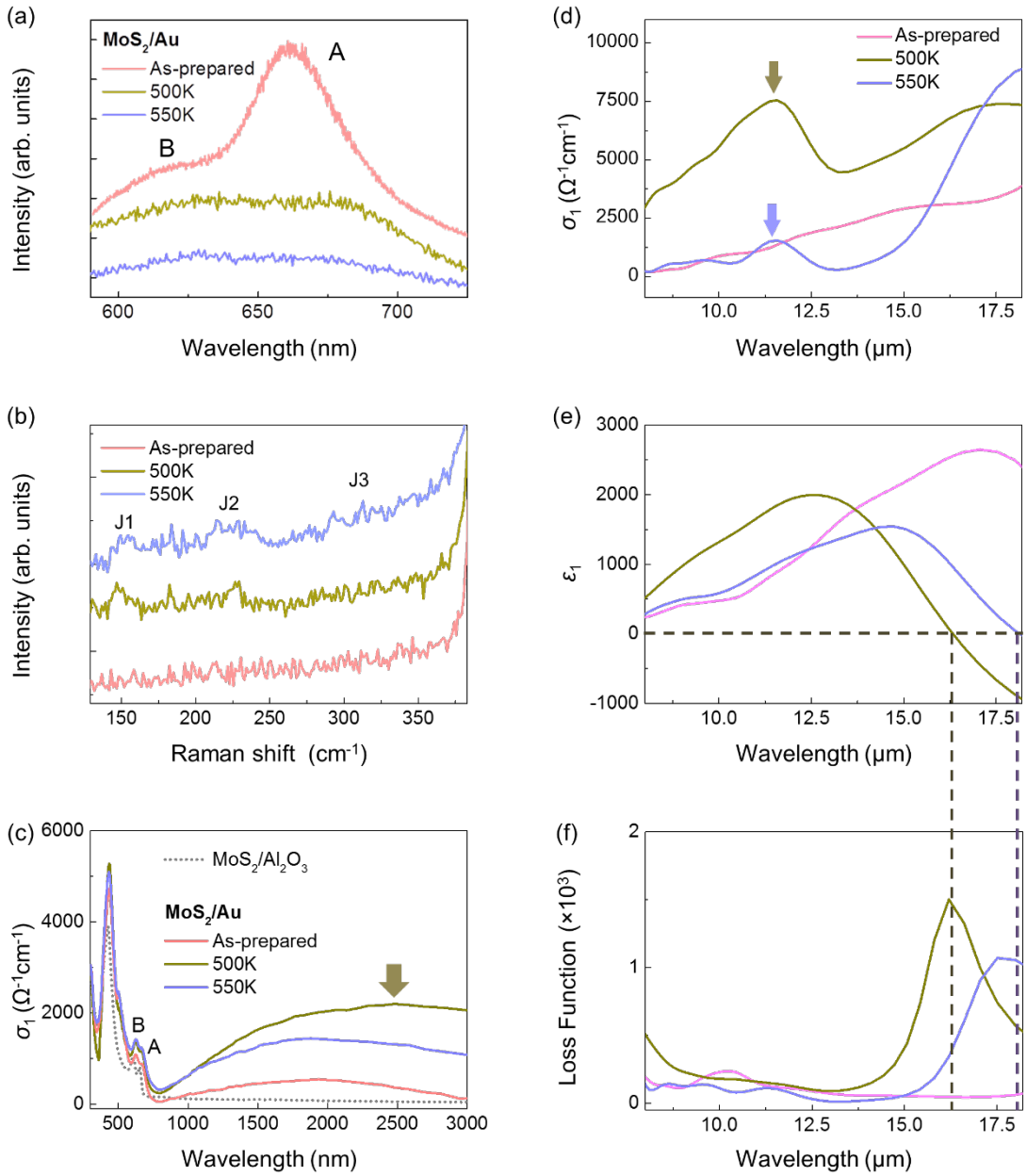

Figure 4. (a) PL data of the monolayer-MoS_2/Au sample, (b) Raman spectra where the J1, J2 and J3 features of 1T'-phase monolayer-MoS_2 are indicated. (c) IR-to-visible range spectroscopic ellipsometry data where the arrow indicates the position of the inverted gap feature of 1T'-phase monolayer-MoS_2/Au. (d) Optical conductivity, σ_1, spectra of monolayer-MoS_2/Au where colour-coded arrows indicate the position of the fundamental gap of 1T'-phase MoS_2/Au after annealing at the respective temperature. (e) Dielectric function, ε_1, and (f) LF spectra of as-prepared monolayer-MoS_2/Au and after annealing at respective temperatures. Intersections of the dashed lines match the zero-crossing positions of the ε_1-spectra (e) and the LF peak positions (f) after annealing at the respective temperature.

Short Summary

New one-dimensional mid-infrared anisotropic plasmons have been observed in the quasi-metallic-phase of WSe_2 and MoS_2 monolayers. In-depth analysis reveals that the long-range inter-chain coupling is responsible for this 1D-charge dynamics and the plasmon energy is dictated by the effects of spin-orbit coupling. This study establishes an inextricable link between the 1D-chain structure and charge dynamics in quasi-metallic-phase 2D transition-metal dichalcogenides.

Keyword
plasmon, anisotropic charge dynamics, phase transition, spin-orbit coupling, electron correlations

Chi Sin Tang, Xinmao Yin*, Ming Yang, Di Wu, Jing Wu, Lai Mun Wong, Changjian Li, Shi Wun Tong, Yung-Huang Chang, Fangping Ouyang, Yuan Ping Feng, Shi Jie Wang, Dongzhi Chi, Mark B. H. Breese, Wenjing Zhang, Andrivo Rusydi, Andrew T. S. Wee*

Anisotropic collective charge excitations in quasi-metallic two-dimensional transition-metal dichalcogenides

ToC figure